Two-photon decay in silver and hafnium atoms

Ilakovac, Ksenofont; Horvat, V.; Krečak, Z.; Jerbić-Zorc, Gorjana; Ilakovac, N.; Bokulić, T.

Two-photon decay in silver and hafnium atoms

K. Ilakovac
Department of Physics, Faculty of Science, University of Zagreb, P.O. Box 162, 41001 Zagreb, Croatia and R. Bošković Institute, P.O. Box 1016, 41001 Zagreb, Croatia

V. Horvat*
Department of Physics, Faculty of Science, University of Zagreb, P.O. Box 162, 41001 Zagreb, Croatia

Z. Krečak
R. Bošković Institute, P.O. Box 1016, 41001 Zagreb, Croatia

G. Jerbić-Zorc
Department of Physics, Faculty of Science, University of Zagreb, P.O. Box 162, 41001 Zagreb, Croatia

N. Ilakovac
R. Bošković Institute, P.O. Box 1016, 41001 Zagreb, Croatia

T. Bokulić
Department of Physics, Faculty of Science, University of Zagreb, P.O. Box 162, 41001 Zagreb, Croatia
(Received 23 August 1991; revised manuscript received 28 February 1992)

The decay of silver and hafnium atoms with a vacancy in the K shell by the emission of photon pairs which continuously share the transition energy was studied. Radioactive decay of ^{109}Cd and of ^{179}Ta was used to generate K-shell vacancy states in silver and hafnium atoms, respectively. A pair of germanium detectors in a 180° geometry and a fast-slow coincidence system with a $(128\times512\times512)$-channel three-parameter pulse-height analyzer were used in the measurements. Two-dimensional spectra of numbers of events as functions of amplitudes of coincident pulses from the two detectors were analyzed. Surface fitting of two-dimensional spectra and curve fitting of sum spectra were applied to deduce the number of events. The differential transition probabilities of $2s\rightarrow1s$, $3s\rightarrow1s$, $3d\rightarrow1s$, and $4sd\rightarrow1s$ two-photon decay per decay of a K-shell vacancy have been determined. For silver they are compared with the results of relativistic self-consistent-field calculations of Mu and Crasemann [Phys. Rev. A **38**, 4585 (1988)] and of Tong, Li, Kissel, and Pratt [Phys. Rev. A **42**, 1442 (1990)]. The results for silver and hafnium are compared with the results of nonrelativistic calculations for hydrogenic silver and hafnium ions. The $3d\rightarrow1s$ two-photon decays show the resonance effect, in accordance with the theoretical predictions.

PACS number(s): 31.30.Jv, 32.30.Rj, 32.80.Wr

I. INTRODUCTION

Removal of an electron from the K shell of a neutral many-electron atom gives rise to very fast transitions, among which are most prominent the emission of $K\alpha$ and $K\beta$ x rays, and of Auger electrons. Higher-order processes are also possible, but they have much smaller transition probabilities. Freund [1] considered the decay of K-shell vacancy states by the simultaneous emission of photon pairs which continuously share the transition energy, the two-photon decay (also named double-photon decay). To the lowest order, it is a second-order process in time-dependent perturbation theory. On the basis of a simple theory he derived the total transition probability of $2s\rightarrow1s$ two-photon decay per decay of a K-shell vacancy in copper of approximately 10^{-6} and concluded that experimental detection of the process was feasible. Bannett and Freund [2] made new calculations of $2s\rightarrow1s$ and $3s\rightarrow1s$ two-photon decay in molybdenum using a nonrelativistic electric-dipole approximation, tabulated wave functions of the Roothaan type, and frozen orbitals. They also reported the results of their measurements of two-photon decay in molybdenum which was excited by a beam of silver x rays. Ilakovac, Tudorić-Ghemo, Bušić, and Horvat [3] measured two-photon decay in xenon atoms. Radioactive ^{131}Cs was used as a generator of xenon atoms with a vacancy in the K shell. They derived the results on $2s\rightarrow1s$, $3s\rightarrow1s$, $3d\rightarrow1s$, and $4sd\rightarrow1s$ two-photon decay, and gave upper limits on $2p_{1/2}\rightarrow1s$, $2p_{3/2}\rightarrow1s$, $3p\rightarrow1s$ and $4p\rightarrow1s$ two-photon decay.

Mu and Crasemann [4] made detailed relativistic self-consistent-field calculations of two-photon decay in xenon atoms. They extended the calculations to two-photon decay in molybdenum and silver atoms [5]. Wu and Li [6] made nonrelativistic self-consistent-field calculations of two-photon decay in krypton, xenon, and radon atoms. Tong, Li, Kissel, and Pratt [7] made detailed relativistic self-consistent-field calculations of two-photon decay in molybdenum, silver, and xenon atoms.

The excited states of hydrogenic (nucleus plus one elec-

tron) systems and the many-electron atoms with a vacancy in an inner shell have many properties in common. This also applies to two-photon decay. The role of occupied electron states as intermediate states in the two-photon decay process was at first uncertain. Guo [8] proved that occupied intermediate electron states are not excluded by the Pauli principle, but act the same way as the unoccupied states. The proof asserted that the inclusion of occupied intermediate states in previous calculations [2,4] was correct. For these reasons it is of interest to compare also the theoretical results for the hydrogenic systems to the experimentally determined values. The theory of $2s \rightarrow 1s$ decay was developed in 1931 by Maria Göppert-Mayer [9] but detailed calculations were made in 1959 by Shapiro and Breit [10]. The nonrelativistic problem of two-photon decay in hydrogenic systems has been solved analytically, first for the $2s \rightarrow 1s$ decay [11,12], and subsequently for transitions among other states which satisfy the two-electric dipole selection rule [13–16].

We report the results of our measurements of two-photon decay in silver and hafnium atoms. Preliminary results on this work were previously reported at conferences [17], but with an erroneously introduced factor of 0.5 [18].

II. APPARATUS

A pair of planar high-purity germanium detectors (supplied by EG and G ORTEC Inc, Oak Ridge, Tennessee) was used for the detection of photons emitted from the radioactive sources. They were placed head-on in a close 180° geometry. Multilayer shields with 1-mm-diam double-taper holes were used to hold the sources centered between the detectors and to reduce the crosstalk. The detectors and a shield with a source were placed in a cylindrical lead shield of 52-mm inner and 80-mm outer diameter.

Nominal size of the detectors was 200-mm^2 area$\times$7 mm-thickness. Energy resolution of the two detectors for 5.9-keV photons was about 230 and 240 eV. The electronic system consisted of a fast-slow coincidence unit and a three-parameter ($128\times512\times512$)-channel analyzer. For each coincidence event ($2\tau=250$ ns) a record was made of the time difference (the time channel, k_0) and of the amplitudes of pulses (nominal time constants of the amplifiers were 4 μs) from the two detectors (the energy channels, k_1 and k_2). The recorded data were analyzed off-line in personal computers. The experimental setup was the same as in the previous measurements of two-photon decay in xenon, except for different electronic adjustments (see Ref. [18] for a more detailed description). Before the start and after the end of each measurement the system was checked for the peak positions and for counting rates in the singles spectra, and calibrated with a high-precision mercury-relay pulse generator.

III. MEASUREMENTS AND ANALYSIS OF DATA ON TWO-PHOTON DECAY IN SILVER

Silver atoms with a vacancy in the K shell were generated in the decay of radioactive ^{109}Cd. In the decay, two processes cause the removal of electrons from the K shells, the electron capture, which proceeds directly to the 39.8-s metastable state in ^{109}Ag at 88 keV, and the electron conversion process. In the decay of ^{109}Cd 81.5% is K capture and in the decay of the ^{109}Ag isomeric state 41.7% is K-electron conversion [19].

^{109}Cd in a 1N HCl solution was acquired from New England Nuclear (Boston, Mass.). A drop of the solution was placed onto a polyethylene sheet. A small piece of pure cellulose paper, cut to a size of approximately 0.4 mm diam, was placed into the drop and the drop was dried. The small piece of radioactive paper was placed between two foils of polyethylene (about 0.06 mm thick) and carefully centered in the hole of the shield. As described above, the shield with the source was placed between two high-purity germanium detectors.

Two series of measurements were made, the first consisted of 21 and the second of 12 measurements. Initial strength of the source of the first 4 measurements of the first series was about 0.8 kBq and of the remaining 17 measurements about 2.2 kBq, the dispersion in either energy branch was close to 60 eV per channel and the shield was made of aluminum with brass inserts. In the second series of measurements the initial strength of the source was about 1.3 kBq, the dispersion 70 eV per channel and the shield was made of brass with gold inserts.

For each measurement total projections of the recorded data onto the k_0 (time), and the k_1 and k_2 (energy) axes were made. The projection spectra were analyzed and positions of characteristic peaks were compared. For each of the two series of measurements the records differing by less than one channel in the peak positions in the region from 9 to 12 keV were accepted. By that criterion only one (the first) measurement of the first series was rejected. All data from the 20 accepted measurements of the first series were formed into one set of data and all data from the 12 measurements of the second series into the second set. Each set was analyzed separately. The total times of collection of data were 1121 and 2118 h for the first and second set, respectively.

A detailed description of the methods of analysis of data on two-photon decay in xenon atoms was given in a previous publication (Ref. [18]). The same methods were adapted for the analysis of data on two-photon decay in silver. Here they are only briefly described. As the measurements lasted for several months, great care was taken to achieve stable operation of the apparatus. In order to avoid effects of small shifts the analysis of data relied entirely on the complete sets of records of the three-parameter data.

Projection of the three-parameter data onto the k_0 axis for various sections of the k_1-k_2 plane yielded the time spectra. They were analyzed with the aim to determine the intervals of k_0 channels which included about 95% of coincidence events. The data in the chosen time intervals were projected onto the k_1-k_2 plane. In this way the tables of in-coincidence numbers of events, the E_1-E_2 energy spectra (one for each of the two sets of data) were obtained. The E_1-E_2 energy spectra were the basis of all subsequent analyses.

Due to the 180° geometry, crosstalk among the two

detectors via germanium K x rays caused prominent peaks in the E_1-E_2 spectra. Absorption of a silver K x ray in the sensitive volume of one detector accompanied by the emission of a K x ray from a germanium atom, escape of the x ray from the detector, its passage through the hole in the shield between the detectors, and its absorption in the second detector caused the crosstalk events [20]. If we denote the energies of K (i.e., $K\alpha_2$, $K\alpha_1$, $K\beta_1$, and $K\beta_2$) x rays of silver by E(Ag Kx), and of germanium by E(Ge Kx), than the energies deposited in the first detector equal E(Ag Kx)$-E$(Ge Kx) and in the second detector E(Ge Kx). We denote these events by

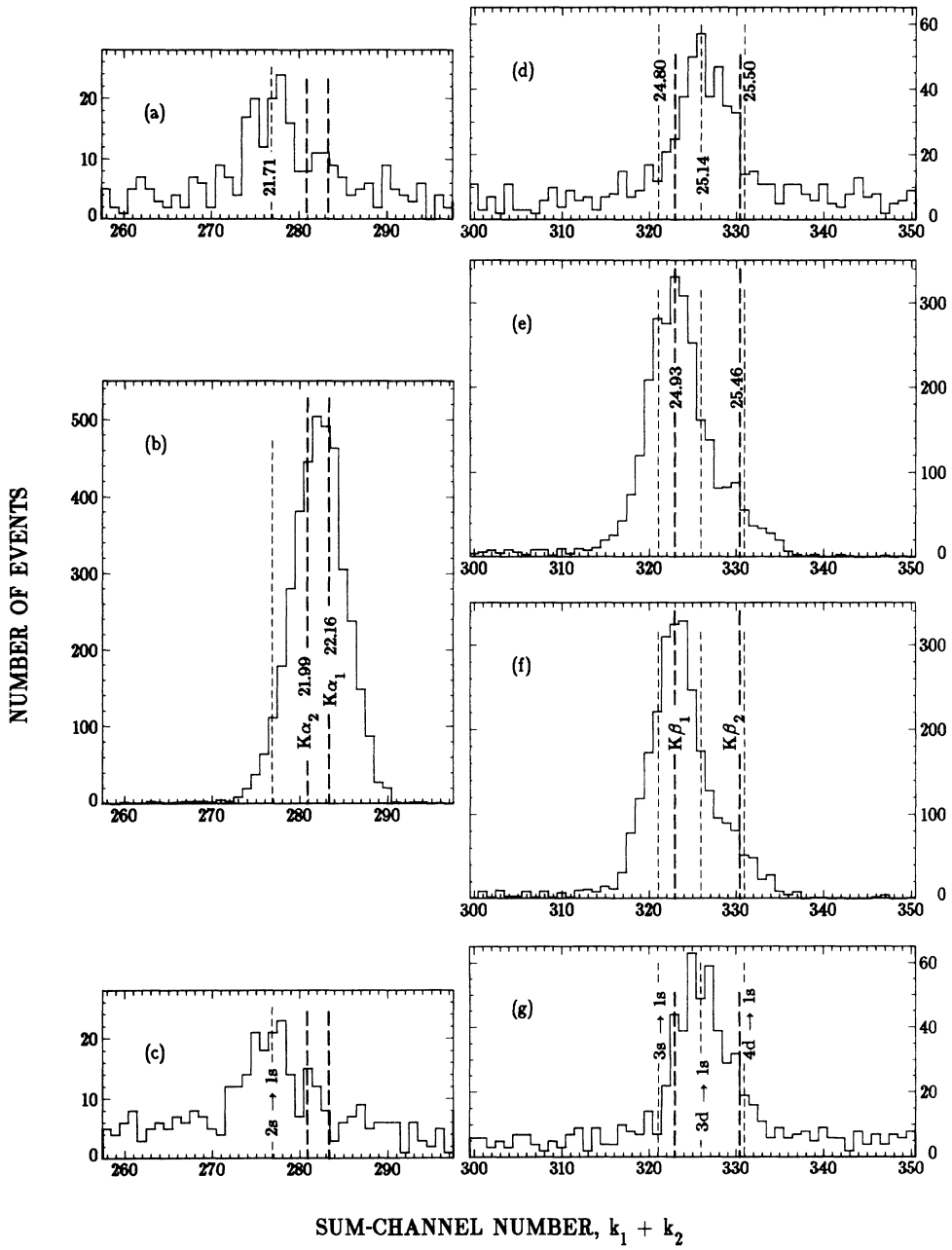

FIG. 1. Sum spectra of sections of the E_1-E_2 spectrum obtained from the data on two-photon decay in silver in the second experiment. In (b) the spectrum obtained by projection of data in a section at the position of the (Ag $K\alpha_{1,2}$–Ge $K\alpha$)–Ge $K\alpha$ two-dimensional peak onto the k_1+k_2 axis is shown. Similarly, (e) and (f) show sum spectra obtained from sections around the (Ag $K\beta_{1,2}$–Ge $K\alpha$)–Ge $K\alpha$ two-dimensional peaks. Sum energies corresponding to the $K\alpha_{1,2}$ and $K\beta_{1,2}$ x rays of silver are indicated by the heavy dashed lines. Sum spectra obtained by projection of data in sections of the ridge due to the $2\rightarrow 1s$ two-photon decay are shown in (a) and (c). The expected position of the peak is shown by the light dashed line. Similarly, sum spectra obtained from the data in sections of the E_1-E_2 spectrum where the higher shell $\rightarrow 1s$ two-photon decay was observed are shown in diagrams (d) and (g). Expected positions of the lines are shown by the light dashed lines. Transition energies are given in keV.

TABLE I. Energies deposited in two germanium detectors by crosstalk events via germanium K x rays for silver K x rays emitted from the source.

Event in one detector	Energy (eV)	Event in the other detector	Energy (eV)
Ag $K\alpha_2$–Ge $K\alpha$	12 114	Ge $K\alpha$	9 876
Ag $K\alpha_2$–Ge $K\beta$	11 010	Ge $K\beta$	10 980
Ag $K\alpha_1$–Ge $K\alpha$	12 287	Ge $K\alpha$	9 876
Ag $K\alpha_1$–Ge $K\beta$	11 183	Ge $K\beta$	10 980
Ag $K\beta_1$–Ge $K\alpha$	15 054	Ge $K\alpha$	9 876
Ag $K\beta_1$–Ge $K\beta$	13 950	Ge $K\beta$	10 980
Ag $K\beta_2$–Ge $K\alpha$	15 584	Ge $K\alpha$	9 876
Ag $K\beta_2$–Ge $K\beta$	14 480	Ge $K\beta$	10 980

(Ag Kx–Ge Kx)–Ge Kx. Table I gives the energies deposited in the two detectors by the crosstalk events. Since the K x rays of silver have a considerably lower energy than those of xenon, the relative positions of the crosstalk peaks in the E_1-E_2 spectra are different. In particular, the (Ag $K\alpha$–Ge $K\beta$)–Ge $K\beta$ crosstalk peaks masked the central region of the $2s \rightarrow 1s$ two-photon decay distribution for silver. The crosstalk peaks allowed a very reliable energy calibration of the energy axes. For that reason linear fitting routines could be applied in the analyses of the two-dimensional energy spectra.

An improvement in the measurements of two-photon decay in silver, in comparison to the study of two-photon decay in xenon atoms [3,18], was the use of lower discriminator thresholds. Reliable determination of the numbers of events due to two-photon decay below the energy of germanium K x rays was possible.

The data due to two-photon decay were observed in the two E_1-E_2 energy spectra as continuous bands along the lines of constant sum energy corresponding to the $2s \rightarrow 1s$, $3s \rightarrow 1s$ $3d \rightarrow 1s$, and $4sd \rightarrow 1s$ transitions. Sum spectra derived from the data in a section around the (Ag $K\alpha_{1,2}$–Ge $K\alpha$)– Ge Kα peaks of an $E_1 - E_2$ spectrum is shown in Fig. 1(b). Sum spectra of sections of the ridge due to the $2s \rightarrow 1s$ two-photon decay are shown in Figs. 1(a) and 1(c). The shift of the peaks in the two latter diagrams is due to the difference of the binding energy of $2s$ and $2p_{1/2,3/2}$ electrons in silver atoms. Similarly, Figs. 1(e) and 1(f) show sum spectra of sections around the (Ag $K\beta_{1,2}$–Ge $K\alpha$)–Ge $K\alpha$ peaks, and Figs. 1(d) and 1(g) sum spectra of sections of the ridges due to the higher shell $\rightarrow 1s$ two-photon decay. Two methods were applied to determine the numbers of events. In one, complex surfaces were fitted to the sections of each of the two E_1-E_2 spectra. Regions around the crosstalk peaks were omitted. In the second method projections of data onto the $k_1 + k_2$ axis were made for several intervals of $x = E/E_0$, the ratio of energy of one photon and of the transition energy of two-photon decay, omitting again the regions around the crosstalk peaks. The one-dimensional spectra were fitted by curves. In either case linear fitting routines were applied, because the energy scales and widths of the peaks were fixed. The numbers of events were derived using equal weights and the errors using $1/n$ weights (one for zero count [21]). The methods are described in more detail in Ref. [18].

An (Ag $K\alpha$–Ge Kx)–GeKx crosstalk event may be accompanied by the absorption of an Ag L x ray in the same detector where the Ge K x ray was absorbed. A coincidence event occurs in which the energy E(Ag Kx)$-E$(Ge Kx) is recorded in one, and the energy E(Ge Kx)$+E$(Ag Lx) in the other detector. We designate these events by (Ag $K\alpha$–Ge Kx)–(Ge Kx+Ag Lx). Since the emission of L x rays following the $K\alpha_1$ or $K\alpha_2$ transitions occurs by filling of $2p_{3/2}$ or $2p_{1/2}$ vacancies, these L x ray transitions are due to electrons originating from $3s$, $3d$, $4s$, $4d$, etc. states. Therefore the sum energies of (Ag $K\alpha$–Ge Kx)–(GeKx+Ag Lx) events fit exactly the sum energies of $3s \rightarrow 1s$, $3d \rightarrow 1s$, $4sd \rightarrow 1s$ two-photon decay events. In the measurements of two-photon decay in xenon atoms [3,18] a small contribution due to this effect was found, and the derivation of the number of counts due to the two-photon decay was made taking this effect into account. In the analysis of results of measurements of two-photon decay in silver atoms, the effect is negligible because of the lower energy of L x rays of silver and their about eight times stronger absorption in the source, air, and the beryllium window. Therefore it was neglected.

IV. MEASUREMENTS AND ANALYSIS OF DATA ON TWO-PHOTON DECAY IN HAFNIUM

Radioactive ^{179}Ta was produced in the cyclotron of the R. Bošković Institute. A rotating copper target, onto which small pieces of high-purity hafnium metal plates were hard soldered, was bombarded by a 14-MeV deuteron beam. Integrated current was about 2.5 mAh. After a cooling period of about two and a half months, separation of ^{179}Ta was made by the following procedure: Filings of the irradiated hafnium metal were dissolved in a mixture of 6 N HCl and 1 N HF. The solution was evaporated from 1.5 to 0.5 ml, 6 M HCl was added to make 2 ml, and the solution was evaporated again to 0.5 ml. A mixture of 12 M HCl and 0.4 M HF was added to make 2 ml and the solution was evaporated to 0.5 ml. The last operation was repeated once and the 12 M HCl plus 0.4 M HF mixture was added to make 3 ml. Next, solvent extraction from the solution was made using diisobutil ketone equilibrated with the 12 M HCl plus 0.4 M HF mixture. Finally, aqueous extraction from the organic solvent was made. The procedure yielded a carrier-free source of ^{179}Ta of a very high radioactive purity. The aqueous solution was dried and the traces of substance were collected using minute specks of glue. When dry, small spherically shaped sources were obtained of diameters of about 0.4 mm. A source was placed between two foils of polyethylene, carefully centered in the hole of a multilayer shield (made of aluminum with copper, tin, and gold inserts), and placed between the two germanium detectors.

Several test runs were made to check the system and to make adjustments. Three measurements were made with a ^{179}Ta source about 3.4 kBq strong. Projections of the three-parameter data onto the k_0, k_1, and k_2 axes were analyzed to check for the consistency of the data. Negli-

gible shifts were found, so the complete records of the three measurements were treated as one set of data. The total time of the collection of the data of the three measurements was about 426 h.

Projection of the three-parameter data from several regions of the k_1-k_2 field yielded the time spectra. They were analyzed to check for the energy dependence of the shifts in timing. A large central region showed negligible shifts of the coincidence peaks, while regions for low values of k_1 or k_2 showed increasingly larger shifts. Therefore, the analysis was limited to the central region, corresponding to the photon energies in either detector above about 17 keV. The time spectrum of the central region was used to select the coincidence region of k_0 channels about ± 2 standard deviations wide. Therefore, about 95% of the coincidence events were included in the subsequent analyses.

As in the analyses of data on two-photon decay in silver, the two-dimensional E_1-E_2 energy spectrum was obtained by projecting onto the k_1-k_2 plane all three parameter data in the accepted interval of time (k_0) channels. All the subsequent analyses were based on the E_1-E_2 spectrum.

The discriminator thresholds were set above the peaks due to the hafnium L x rays. Otherwise a high coincidence rate would have required the use of a much weaker source. In this way coincidences due to the crosstalk among the detectors via germanium K x rays were also eliminated. Since no isolated two-dimensional peaks were observed in the analyzed region of data, energy calibration was based on sum spectra. The sum spectra were made for several sections of the k_1-k_2 field, for lower values and for higher values of k_1 with the aim to check whether the energies per channel on the k_1 and k_2 axes were equal. Namely, the two-photon decay events appear in the E_1-E_2 spectrum as ridges at constant sum energy. If the energies per channel on the k_1 and k_2 axes are equal, the data lay along lines at constant values of k_1+k_2, and the sum spectra of the sections of the E_1-E_2 spectrum show no shifts. The sum spectra were analyzed assuming the presence of peaks due to the $2s \rightarrow 1s$, $3s \rightarrow 1s$, $3d \rightarrow 1s$, and $4sd \rightarrow 1s$ two-photon decay, and peaks due to the absorption of hafnium K x rays in one detector accompanied by crosstalk among the germanium detectors via the Compton effect. The results have shown a close equality of the scales on the k_1 and k_2 axes. Two separate measurements were made, one before and the other after the above-described measurements, with a weaker source and lower discriminator thresholds. Since the pulses from the absorption of L x rays triggered the discriminators, multiple two-dimensional peaks were observed due to the coincidences of K and L x rays of hafnium. Two-dimensional fitting routines were applied to determine the positions of the peaks and the energy scales on the k_1 and k_2 axes. The energies per channel on the k_1 and k_2 axes thus determined were in a very good agreement, and when recalculated to the sum-energy scale, a very good agreements was obtained with the scale derived from the sum spectra. In this way stability of the system and the close equality of the energy scales on the k_1 and k_2 axes were checked.

As mentioned above, coincidence events due to the crosstalk via backscattered Compton radiation were observed in the E_1-E_2 spectrum. A K x ray of hafnium emitted from the source may get backscattered by the Compton effect in the sensitive volume of one germanium detector and the secondary Compton photon may escape from the detector. Energy deposited in the detector is equal to the sum of the electron binding energy and electron kinetic energy. If the secondary Compton photon passes through the hole in the shield and is absorbed in the sensitive volume of the other detector, a coincidence event occurs. Sum energy of the two events is equal to the energy of the primary K x ray of hafnium, because the probability of escape of any other secondary radiation from either detector is very low. Compton backscattering of a hafnium $K\alpha_1$ x ray on a loosely bound electron would cause an energy transfer to the electron of about 10 keV, and the backscattered secondary photon would have an energy of about 45.8 keV. Scattering on loosely bound electrons is most probable, but such events do not yield coincidences because of the discriminator thresholds. Compton scattering on strongly bound electrons causes a broad energy distribution of the backscattered Compton radiation. Due to this effect coincidence events from the crosstalk via backscattered Compton radiation were recorded in the measurement, particularly in the regions of low-k_1 and of low-k_2 channels.

Sum spectrum from a broad region of the k_1-k_2 field is shown in Fig. 2. The range of the parameter $x=E/E_0$,

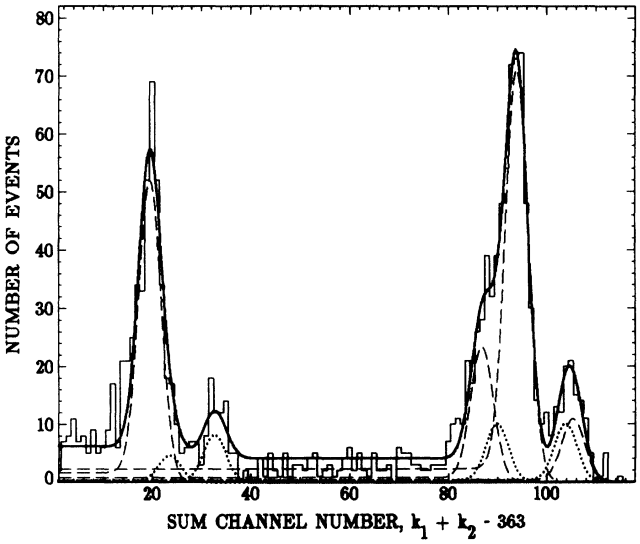

FIG. 2. The histogram shows the sum spectrum made from the data in a central region of the E_1-E_2 two-dimensional spectrum of the hafnium experiment, for $x=E/E_0$ in a range between about 0.35 to about 0.65. The dashed curves show (in the order from the left to the right) the peaks of the fitting functions due to the $2s \rightarrow 1s$, $3s \rightarrow 1s$, $3d \rightarrow 1s$, and $4sd \rightarrow 1s$ two-photon decay. The dotted curves show (again in the order from the left to the right) the fitting functions due to the crosstalk via backscattered Compton radiation from the $K\alpha_2$, $K\alpha_1$, $K\beta_1$, and $K\beta_2$ x rays of hafnium. The heavy solid line shows the sum of the above fitting functions and of a constant background.

i.e., of the ratio of energy of one photon from two-photon decay to the transition energy, is from about 0.35 to about 0.65. The sum spectrum was analyzed by a minimum χ^2 routine with the aim to determine the sum-energy scale and the peak widths. The component functions in the sum spectrum were assumed to be the peaks due to the $2s \rightarrow 1s$, $3s \rightarrow 1s$, $3d \rightarrow 1s$, and $4sd \rightarrow 1s$ two-photon decay and the peaks due to crosstalk via backscattered Compton radiation from the $K\alpha_2$, $K\alpha_1$, $K\beta_1$, and $K\beta_2$ x rays of hafnium. Each peak was represented by a discrete function that was calculated by integration of the Gaussian function over the widths of single channels, channel by channel. Also, each peak was assumed to have a "left shoulder" which was represented by an integral Gaussian function. Variable parameters of the fit were two energy points (the positions of the $2s \rightarrow 1s$ and $3d \rightarrow 1s$ sum peaks), amplitudes of the $2s \rightarrow 1s$, $3s \rightarrow 1s$, $3d \rightarrow 1s$, and $4sd \rightarrow 1s$ peaks, amplitude of the $K\alpha_1$ crosstalk peak, gradient of the assumed linear function representing the efficiency of the measuring system for the detection of crosstalk event on energy, a parameter representing the widths of the peaks, the relative height of the "left shoulder," and a constant background. Resulting functions of the fitting procedure, i.e., the component functions and the function of the fit, are shown in Fig. 2 by curves.

Two methods of analysis of the E_1-E_2 spectrum were applied: fitting of a surface to the central region that was subdivided into several sections, and the fitting of curves to the sum spectra that were made by projecting the data in the E_1-E_2 spectrum onto the k_1+k_2 axis. Since the energy scales and widths of the peaks were fixed, linear routines were applied. The two methods of analysis are described in more detail in Ref. [18]. The fitting function was different in that the ridges (in surface fitting) and the peaks (in curve fitting) in addition to the $2s \rightarrow 1s$, $3s \rightarrow 1s$, $3d \rightarrow 1s$, and $4sd \rightarrow 1s$ lines, also included the crosstalk lines due to Compton backscattering of K x rays of hafnium. Actually, the functions of the fit were the same as those described above for the nonlinear fitting of the sum spectrum that was the basis of the energy scale. The numbers of events were derived using equal weights and the errors using $1/n$ weights (1 for zero count [21]). The two methods yielded the numbers of events, Δn, due to the $2s \rightarrow 1s$, $3s \rightarrow 1s$, $3d \rightarrow 1s$, and $4sd \rightarrow 1s$ two-photon decay for a number of energies of one photon of the pair. A good agreement between the two sets of results was obtained. The results of the curve fits seem to be more reliable.

V. RESULTS AND DISCUSSION

The differential transition probabilities of the two-photon decay per decay of a K-shell vacancy were calculated from the formula [18]

$$\frac{1}{W_K}\left[\frac{dW}{dE\ d\Omega_1 d\Omega_2}\right]_{\theta=\pi} = \frac{\Delta n/\Delta E}{n_K \epsilon_1 \epsilon_2 \epsilon_C \Delta\Omega_1 \Delta\Omega_2 F}$$

(previous factor of 0.5 on the right-hand side of the equation is omitted), where Δn is the number of events due to two-photon decay in an energy interval ΔE, n_K is the number of K-shell vacancies generated in the source during the measurement, ϵ_1 and ϵ_2 are the peak efficiencies of the detectors, ϵ_C is the coincidence efficiency, $\Delta\Omega_1$ and $\Delta\Omega_2$ are the solid angles of the detectors subtended from the source, and F is a correction factor (equal to the average value over solid angles of the two detectors of the product of the angular correlation function, of the photon-attenuation factors, and of the probabilities of total-energy absorption in germanium [18]).

In the measurements on two-photon decay in silver atoms the solid angles of the detectors were $\Delta\Omega_1 = 1.61$ sr and $\Delta\Omega_2 = 1.57$sr, the coincidence efficiency was $\epsilon_C = 0.95$, and the peak efficiencies of the detectors were $\epsilon_1 = \epsilon_2 = 0.95$.

The results on relative differential transition probabilities of $2s \rightarrow 1s$ $3s \rightarrow 1s$, $3d \rightarrow 1s$, and $4sd \rightarrow 1s$ two-photon decay in silver atoms are given in Tables II, III, IV, and V, and are shown in Figs. 3–6. The available theoretical results are also shown in the figures. The dashed curves in Figs. 3–6 show the results of nonrelativistic electric-pole approximation for hydrogenic silver ions. The dashed curve in Fig. 3 was calculated from the results of Shapiro and Breit [10], and from the formulas of Zon and Rapoport [11] and of Klarsfeld [12], which agree completely. The dashed curves in Figs. 4 and 5 were calculated from the results of Florescu [14] and of Tung, Ye, Salamo, and Chan [13] (which closely agree). The dashed curve in Fig. 6 was calculated from the results of calculations of Tung, Ye, Salamo, and Chan [13]. The solid curves in Figs. 3–5 show the results of relativistic self-consistent-field calculations of Mu and Crasemann [5] and of Tong, Li, Kissel, and Pratt [7]. The results of the two groups for the $3s \rightarrow 1s$ two-photon decay closely agree, so the curves in Fig. 4 overlap. Their results for $3d \rightarrow 1s$ two-photon decay show a considerable difference as can be seen in Fig. 5 [curves (*b*) and (*c*)]. In the derivation of all theoretical results the decay rate of the K-shell vacancy in silver atoms was assumed to have the value $W_K = 9.80 \times 10^{15}\ \mathrm{s}^{-1}$.

In the measurements of two-photon decay in hafnium atoms the solid angles of the detectors were $\Delta\Omega_1 = 1.41$ sr and $\Delta\Omega_2 = 1.45$ sr, the coincidence efficiency was $\epsilon_C = 0.95$, and the peak efficiencies of the detectors were $\epsilon_1 = \epsilon_2 = 0.90$.

TABLE II. Relative differential transition probabilities of $2s \rightarrow 1s$ two-photon decay in silver in units of $10^{-9}\ \mathrm{keV}^{-1}\mathrm{sr}^{-2}$ at $\theta = 180°$. The transition energy is $E_0 = 21.708$ keV.

First measurement		Second measurement	
$x = E/E_0$	$\frac{1}{W_K}\frac{d^3W}{dE\,d\Omega_1 d\Omega_2}$	$x = E/E_0$	$\frac{1}{W_K}\frac{d^3W}{dE\,d\Omega_1 d\Omega_2}$
0.303	4.58±2.12	0.279	6.44±1.74
0.358	8.54±1.62	0.337	6.84±1.18
0.414	4.54±1.42	0.395	7.12±1.44
0.587	6.30±1.40	0.608	4.96±1.26
0.643	6.54±1.56	0.666	6.22±1.62
0.699	2.16±1.86	0.724	4.78±1.52

TABLE III. Relative differential transition probabilities of $3s \rightarrow 1s$ two-photon decay in silver in units of 10^{-9} keV^{-1} sr^{-2} at $\theta = 180°$. The transition energy is $E_0 = 24.797$ keV.

First measurement		Second measurement	
$x = E/E_0$	$\frac{1}{W_K}\frac{d^3W}{dE\,d\Omega_1 d\Omega_2}$	$x = E/E_0$	$\frac{1}{W_K}\frac{d^3W}{dE\,d\Omega_1 d\Omega_2}$
0.265	1.12±3.08	0.244	0.24±1.76
0.314	0.64±1.72	0.295	0.98±1.20
0.362	0.32±1.40	0.346	1.36±1.78
0.411	2.96±2.48	0.397	1.96±1.66
0.460	3.44±2.76	0.448	2.08±2.24
0.500	4.04±1.40	0.500	0.80±1.36
0.639	1.76±1.70	0.555	1.90±1.42
0.687	1.04±1.72	0.606	3.88±1.62
0.736	1.10±1.76	0.657	-1.20±1.28
		0.708	0.98±1.18
		0.759	-1.00±1.74

TABLE IV. Relative differential transition probabilities of $3d \rightarrow 1s$ two-photon decay in silver in units of 10^{-9} keV^{-1} sr^{-2} at $\theta = 180°$. The transition energy is $E_0 = 25.144$ keV.

First measurement		Second measurement	
$x = E/E_0$	$\frac{1}{W_K}\frac{d^3W}{dE\,d\Omega_1 d\Omega_2}$	$x = E/E_0$	$\frac{1}{W_K}\frac{d^3W}{dE\,d\Omega_1 d\Omega_2}$
0.261	16.08±2.54	0.241	14.20±1.78
0.309	9.36±1.98	0.291	8.48±1.22
0.357	7.88±1.34	0.341	6.66±1.22
0.406	5.98±3.76	0.391	6.58±1.60
0.454	10.50±3.84	0.441	6.74±1.14
0.500	6.54±1.06	0.500	7.64±1.14
0.548	5.48±3.80	0.561	6.18±1.30
0.596	9.50±3.64	0.611	6.20±1.62
0.644	6.94±1.30	0.661	9.96±1.28
0.692	10.68±1.36	0.712	10.28±1.20
0.740	15.44±1.68	0.762	15.16±1.74

TABLE V. Relative differential transition probabilities of $4sd \rightarrow 1s$ two-photon decay in silver in units of 10^{-9} keV^{-1} sr^{-2} at $\theta = 180°$. The transition energy is $E_0 = 25.480$ keV.

First measurement		Second measurement	
$x = E/E_0$	$\frac{1}{W_K}\frac{d^3W}{dE\,d\Omega_1 d\Omega_2}$	$x = E/E_0$	$\frac{1}{W_K}\frac{d^3W}{dE\,d\Omega_1 d\Omega_2}$
0.258	3.84±2.58	0.238	2.44±1.48
0.305	1.90±1.36	0.287	1.42±1.04
0.353	1.00±1.18	0.337	0.48±1.08
0.400	3.70±2.52	0.386	-0.52±1.36
0.448	0.02±2.44	0.436	1.32±1.18
0.500	0.40±0.90	0.500	-0.26±0.92
0.601	-0.60±2.24	0.567	-0.80±1.18
0.650	2.18±1.14	0.616	-0.14±1.34
0.696	1.40±1.16	0.666	-0.90±1.10
0.743	1.32±1.48	0.716	1.94±0.98
		0.765	2.46±1.46

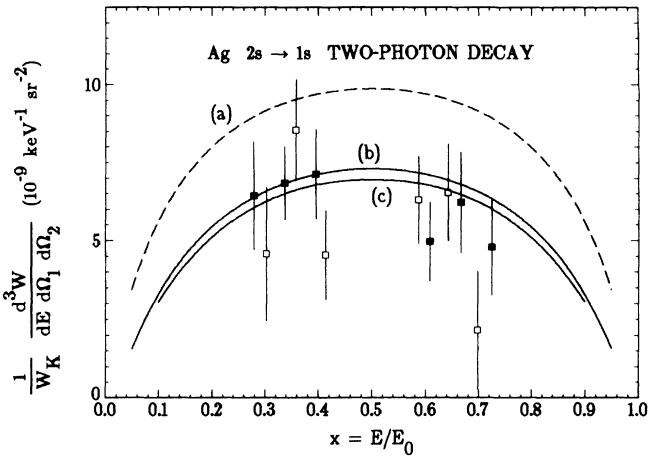

FIG. 3. Relative differential transition probabilities of $2s \rightarrow 1s$ two-photon decay in silver at 180°. Experimental results from the first and second measurements are shown by hollow and full squares, respectively. The dashed curve (*a*) shows the results derived from expressions of Zon and Rapoport [11] for hydrogenic silver ions. The solid curves show the results of relativistic self-consistent-field calculations of Mu and Crasemann [5] [curve (*b*)] and of Tong, Li, Kissel, and Pratt [7] [curve (*c*)].

The results on relative differential transition probabilities of $2s \rightarrow 1s$, $3s \rightarrow 1s$, $3d \rightarrow 1s$, and $4sd \rightarrow 1s$ two-photon decay in hafnium atoms are given in Tables VI, VII, VIII, and IX, and shown in Figs. 7–10. Total transition probability of decay of a K-shell vacancy in hafnium atoms was assumed to have the value $W_K = 5.24 \times 10^{16}$ s^{-1}.

Figures 3–10 in this paper and Figs. 8–11 in Ref. [18] illustrate best the present status of investigation of two-

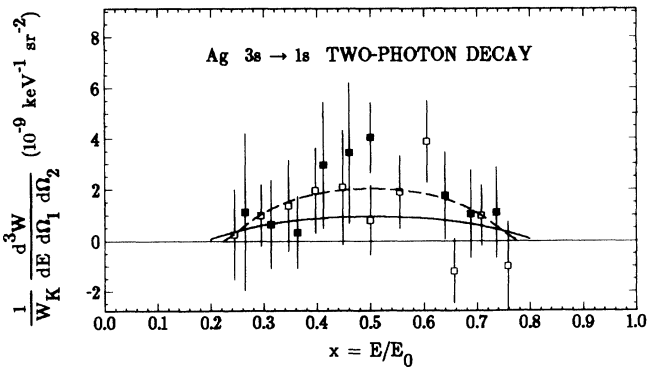

FIG. 4. Relative differential transition probabilities of $3s \rightarrow 1s$ two-photon decay in silver at 180°. Experimental results from the first and second measurements are shown by hollow and full squares, respectively. The dashed curve shows the results derived from expressions of Florescu [14] for hydrogenic silver ions. The solid curve shows the results of relativistic self-consistent-field calculations of Mu and Crasemann [5] and of Tong, Li, Kissel, and Pratt [7].

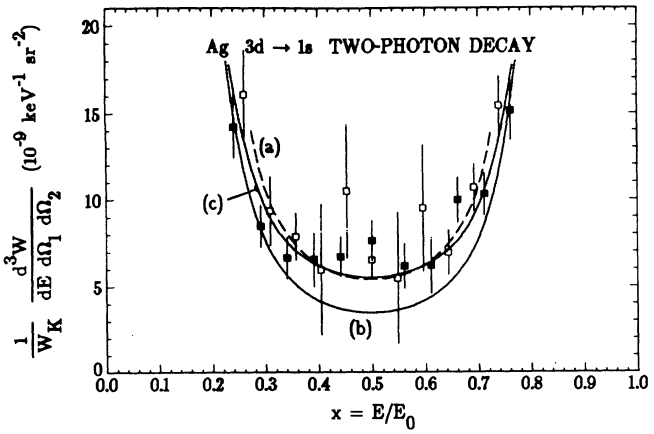

FIG. 5. Relative differential transition probabilities of $3d \rightarrow 1s$ two-photon decay in silver at 180°. Experimental results from the first and second measurements are shown by hollow and full squares, respectively. The dashed curve (*a*) shows the results derived from expressions of Florescu [14] for hydrogenic silver ions. The solid curves show the results of relativistic self-consistent-field calculations of Mu and Crasemann [5] [curve (*b*)] and of Tong, Li, Kissel, and Pratt [7] [curve (*c*)].

photon decay in heavy atoms with a vacancy in the K shell. Further theoretical work and more accurate measurements are required to clear up many of the remaining problems. The rise of the differential transition probability of the $3d \rightarrow 1s$ two-photon decay for increasingly asymmetric partition of energy among the two photons (i.e., for increasing values of $|x-0.5|$) is considered to be the experimental proof of the predicted resonance effect

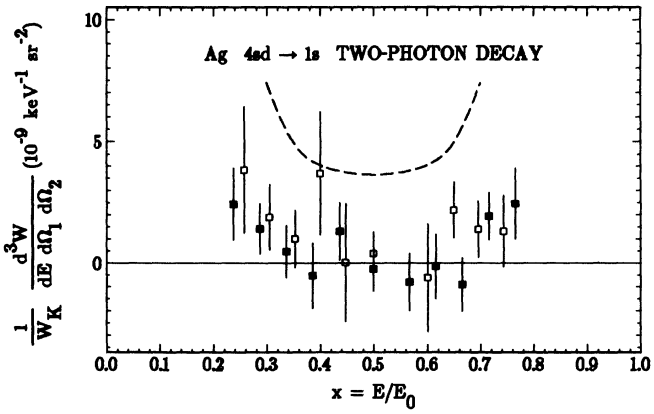

FIG. 6. Relative differential transition probabilities of $4sd \rightarrow 1s$ two-photon decay in silver at 180°. Experimental results from the first and second measurements are shown by hollow and full squares, respectively. The dashed curve shows the values derived from results of Tung, Ye, Salamo, and Chan [13] for hydrogenic silver ions.

TABLE VI. Relative differential transition probabilities of $2s \rightarrow 1s$ two-photon decay in hafnium atoms in units of 10^{-9} keV^{-1} sr^{-2} at $\theta = 180°$. The transition energy is $E_0 = 54.079$ keV.

$x = E/E_0$	$\frac{1}{W_K}\frac{d^3W}{dE\,d\Omega_1 d\Omega_2}$
0.330	2.52±0.63
0.378	4.47±0.73
0.426	3.48±0.62
0.474	4.41±0.65
0.523	4.68±0.68
0.571	4.49±0.70
0.619	4.90±0.75
0.667	2.93±0.65

TABLE VII. Relative differential transition probabilities of $3s \rightarrow 1s$ two-photon decay in hafnium atoms in units of 10^{-9} keV^{-1} sr^{-2} at $\theta = 180°$. The transition energy is $E_0 = 62.750$ keV.

$x = E/E_0$	$\frac{1}{W_K}\frac{d^3W}{dE\,d\Omega_1 d\Omega_2}$
0.395	2.00±0.62
0.436	1.42±0.56
0.478	2.31±0.76
0.519	1.93±0.65
0.561	1.92±0.75
0.602	2.74±0.68

TABLE VIII. Relative differential transition probabilities of $3d \rightarrow 1s$ two-photon decay in hafnium atoms in units of 10^{-9} keV^{-1} sr^{-2} at $\theta = 180°$. The transition energy is $E_0 = 63.667$ keV.

$x = E/E_0$	$\frac{1}{W_K}\frac{d^3W}{dE\,d\Omega_1 d\Omega_2}$
0.355	10.16±1.17
0.396	6.48±0.88
0.437	5.23±0.79
0.478	4.90±0.86
0.519	6.56±0.94
0.560	6.38±0.97
0.601	6.38±0.95
0.642	7.61±1.01

TABLE IX. Relative differential transition probabilities of $4sd \rightarrow 1s$ two-photon decay in hafnium atoms in units of 10^{-9} keV^{-1} sr^{-2} at $\theta = 180°$. The transition energy is $E_0 = 65.130$ keV.

$x = E/E_0$	$\frac{1}{W_K}\frac{d^3W}{dE\,d\Omega_1 d\Omega_2}$
0.399	1.34±0.39
0.439	1.43±0.49
0.479	1.24±0.48
0.519	1.48±0.44
0.559	1.34±0.50
0.599	2.16±0.48

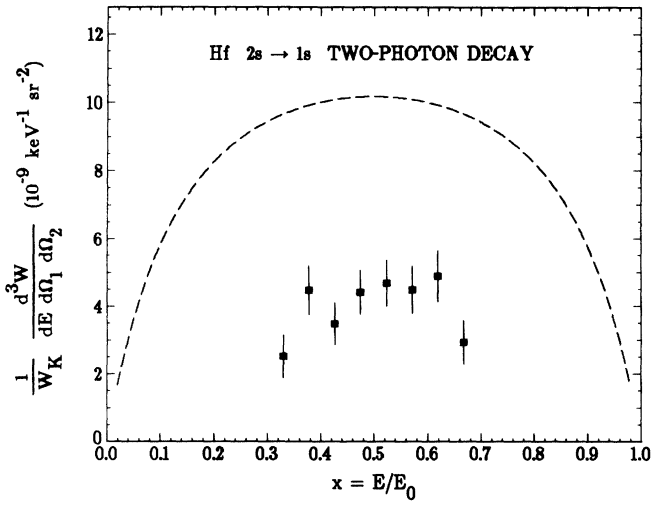

FIG. 7. Relative differential transition probabilities of $2s \rightarrow 1s$ two-photon decay in hafnium at 180°. Experimental results are shown by full squares. The dashed curve shows the results derived from the expressions of Zon and Rapoport [11], and Klarsfeld [12] for hydrogenic hafnium ions.

[2,4]. If the occupied states, particularly the $2p$ state of atoms with a K-shell vacancy, did not take part as intermediate states in the two-photon decay processes, the differential transition probability would show a maximum at $x = 0.5$. Therefore, we may conclude, as predicted by theory, the occupied as well as unoccupied electron states take part as intermediate states in the two-photon decay process. An indication of the effect is also seen in the $4sd \rightarrow 1s$ two-photon decay spectrum of silver, Fig. 6, in which only the $4d \rightarrow 1s$ two-photon decay is expected to show the resonance effect in the observed energy region.

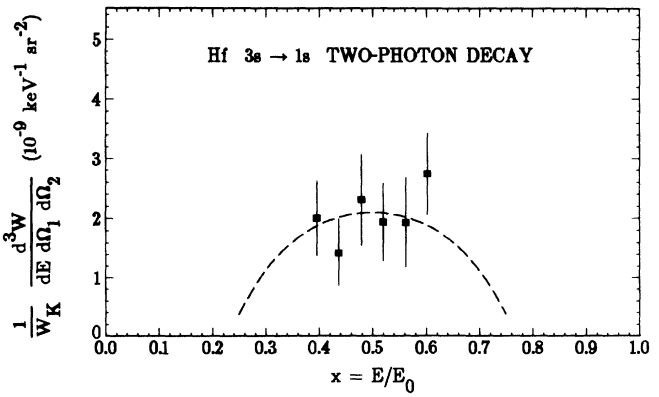

FIG. 8. Relative differential transition probabilities of $3s \rightarrow 1s$ two-photon decay in hafnium at 180°. Experimental results are shown by full squares. The dashed curve shows the results derived from the expressions of Florescu [14,16] and from the results of Tung, Ye, Salamo, and Chan [13] for hydrogenic hafnium ions.

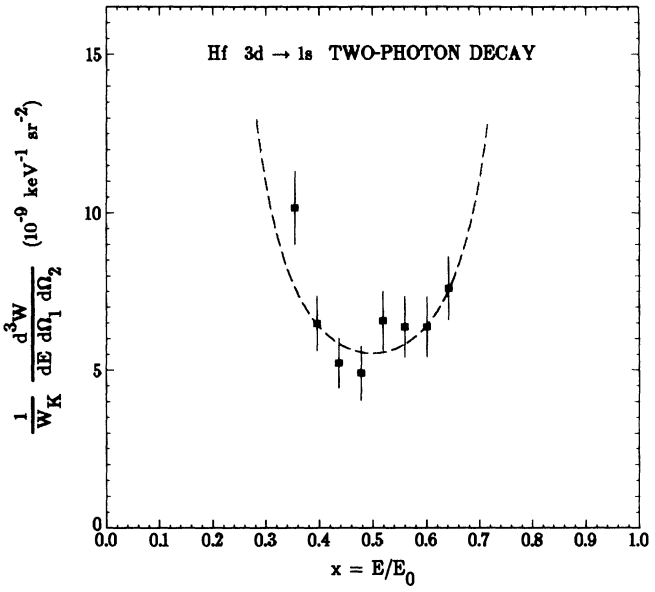

FIG. 9. Relative differential transition probabilities of $3d \rightarrow 1s$ two-photon decay in hafnium at 180°. Experimental results are shown by full squares. The dashed curve shows the results derived from the expressions of Florescu [14,16] and from the results of Tung, Ye, Salamo, and Chan [13] for hydrogenic hafnium ions.

ACKNOWLEDGMENTS

The authors wish to express their gratitude to Professor B. Crasemann and Dr. X. Mu, and to Professor R. H. Pratt for discussions on the theoretical aspects of the two-photon decay, and to Professor Viorica Florescu for sending the results of their calculations on differential

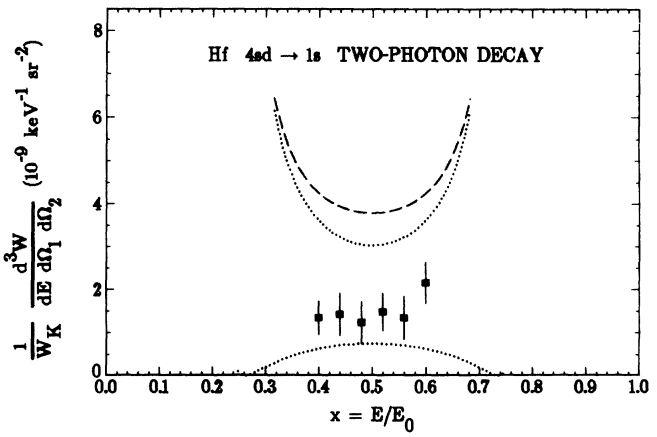

FIG. 10. Relative differential transition probabilities of $4sd \rightarrow 1s$ two-photon decay in hafnium at 180°. Experimental results are shown by full squares. The lower and upper dotted curves show the results serived from the expressions of Florescu [16,18] and from the results of Tung, Ye, Salamo, and Chan [13] for hydrogenic hafnium ions for $4s \rightarrow 1s$ and $4d \rightarrow 1s$ two-photon decay, respectively. The dashed curve shows the sum of the two results.

transition probabilities for two-photon decay in one-electron systems. Many thanks are due to Mr. J. Pfeiffer and Dr. K. Riepe, Forschungszentrum, Jülich, Germany, for giving us a hafnium plate of high purity. The help of Mr. K. Kovačević with the detectors, and of Dr. N. Bogunović, Dr. D. Gamberger, and Dr. Z. Marić of the electronics group of the R. Bošković Institute with the electronics is warmly acknowledged. This work was in part financially supported by the Ministry of Science, Technology, and Informatics of the Republic of Croatia, and by the U.S. National Science Foundation (Project No. PN-734).

---

*Present address: Cyclotron Institute, Texas A & M University, College Station, TX 77843.

[1] I. Freund, Phys. Rev. A **7**, 1849 (1973).
[2] Y. Bannett and I. Freund, Phys. Rev. Lett. **49**, 539 (1982): Phys. Rev. A **30**, 299 (1984).
[3] K. Ilakovac, J. Tudorić-Ghemo, B. Bušić, and V. Horvat, Phys. Rev. Lett. **56**, 2469 (1986).
[4] X. Mu and B. Crasemann, Phys. Rev. Lett. **57**, 3039 (1986).
[5] X. Mu and B. Crasemann, Phys. Rev. A **38**, 4585 (1988).
[6] Y.-J. Wu and J.-M. Li, J. Phys. B **21**, 1509 (1988).
[7] X.-M. Tong, J.-M. Li, L. Kissel, and R. H. Pratt, Phys. Rev. A **42**, 1442 (1990).
[8] D. S. Guo, Phys. Rev. A **36**, 4267 (1987).
[9] M. Göppert-Mayer, Ann. Phys. (Leipzig) **9**, 273 (1931).
[10] J. Shapiro and G. Breit, Phys. Rev. **113**, 179 (1959).
[11] B. A. Zon and L. P. Rapoport, Pis'ma Zh. Eksp. Teor. Fiz. **7**, 70 (1968) [JETP Lett. **7**, 52 (1968)].
[12] S. Klarsfeld, Phys. Lett. **30A**, 382 (1969).
[13] H. Tung, X. M. Ye, G. J. Salamo, and F. T. Chan, Phys. Rev. A **30**, 1175 (1984).
[14] V. Florescu, Phys. Rev. A **30**, 2441 (1984).
[15] A. Costescu, I. Brândus, and N. Mezinescu, J. Phys. B **18**, L11 (1985).
[16] V. Florescu, S. Patrascu, and O. Stoican, Phys. Rev. A **36**, 2155 (1987).
[17] K. Ilakovac, V. Horvat, and Z. Krečak (unpublished); K. Ilakovac, B. Bušić, J. Tudorić-Ghemo, and V. Horvat, J. Phys. (Paris) Colloq. **48**, C9-613 (1987); K. Ilakovac, in *X-Ray and Inner-Shell Processes,* Proceedings of the Fifteenth International Conference on X-ray and Inner-shell Processes, Knoxville, Tennessee, 1990, AIP Conf. Proc. No. 215, edited by T. A. Carlson, M. O. Krause, and S. T. Manson (AIP, New York, 1990), p. 498.
[18] K. Ilakovac, J. Tudorić-Ghemo, and S. Kaučić, Phys. Rev. A. **44**, 7392 (1991).
[19] *Table of Isotopes,* 7th ed., edited by C. M. Lederer and V. S. Shirley (Wiley, New York, 1978).
[20] K. Ilakovac, J. Tudorić-Ghemo, V. Horvat, N. Ilakovac, S. Kaučić, and M. Vesković, Nucl. Instrum. Methods A **245**, 467 (1986).
[21] P. R. Bevington, *Data Reduction and Error Analysis for the Physical Sciences* (McGraw-Hill, New York, 1969).